ADVANCES IN TEST MEASUREMENT
Vol. 5

isa conference

INTRODUCTION

The Test Measurement Division of ISA proudly presents Advances in Test Measurement; Volume 5, which is the proceedings of the 5th International ISA Symposium on Test Measurement, held in conjunction with the 23rd Annual ISA Conference. In keeping with the conference highlight, "New Technologies in Instrumentation," the papers assembled in this proceedings in general, reflect the newest in measurement technology. To help bring these new advancements in technology into proper perspective, several sessions also programmed state-of-the-art and tutorial papers.

It has always been the intent of the Test Measurements Division to bring before the conference, the latest that has been done throughout the immediate past in the field of test measurement technology. To this extent it has been considered extremely important to bring together the man with a measurement problem and the man who may have an answer to that problem. Even if the encounter doesn't provide an answer, it can at least stimulate the thinking necessary to bring it about, rather than expending excessive effort in pedantic rhetoric or extensive review coupled with a rigid and formal format of presentation. The timeliness of the material presented, together with a free exchange of ideas, is more important than the often over-emphasized "classic" nature of the material. Consequently, some papers in these proceedings may be of only fleeting importance, while others may be extensive, lasting works of authority. However, at the time of presentation, each paper represented measurement problems which were of importance to a group or groups of individuals working in that particular discipline.

The papers cover a broad range of measurement disciplines extending from strain, shock vibration measurements; through temperature, heat flux, and thermophysical property measurements; to electro-optical measurements and measurements for nondestructive testing. In addition, four workshop sessions covering "Vibration Measurements" and four workshop sessions covering "Strain Gage Applications and Techniques" were conducted by manufacturers' representatives.

It should be obvious to anyone who attended the symposium or who reviews these proceedings that the papers are the result of extensive effort on the part of many individuals. In addition to the time invested by the many authors who prepared the papers, endless hours were spent in developing the sessions, reviewing manuscripts, together with the planning and organizing time that is required to program a symposium of this magnitude. I offer my sincerest thanks to those who participated to make this symposium a reality, and I hope that each may be rewarded by a sense of accomplishment that will encourage others to join with us in future symposia.

Dieter Rall*, Director
ISA Test Measurements Division

*Trans-Met Engineering, La Habra, California.

TABLE OF CONTENTS

INTRODUCTION

68-501

LONG LINE WIDE-BAND USE OF THE ZERO DRIVE

By: Alfred G. Ratz, MB Electronics

AUTHOR

The author obtained his Ph.D. degree in 1951, for development work on digital computers. Subsequently he was Systems Section Manager, Air Armament Department, Canadian Westinghouse. Moving to the United States, he was Chief Engineer, first of the Applied Science Corporation of Princeton and then of the Ortholog Division of Gulton Industries. He is presently Chief Engineer at MB Electronics, New Haven, Connecticut.

SUMMARY

The zero-drive principle was conceived as a method of overcoming certain basic defects of charge and voltage instrumentation amplifiers. These defects are related to the influence of the input cable on amplifier performance: e.g., increased noise and cross-talk effects with increased cable length. The frequency range of original interest was that associated with conventional vibration and acoustic work. However, the principle can be extended to deal with signals having spectra approaching the video, even when the length of cable between piezo-electric transducer and amplifier is very long.

In this paper, the basic theory is outlined, covering the extended use of the zero-drive. The essential design relationships are also developed. Experimental results are described, confirming the theory.

THE ZERO DRIVE PRINCIPLE

The zero drive amplifier was originally developed for use with self-generating transducers of the piezoelectric type[1]. Its basic principle has been described elsewhere[2], and can be summarized briefly, using the simplified schematic of Figure 1.

The signal from a self-generating transducer is fed directly into the input of a field-effect transistor (FET). This transistor is part of an integrated circuit, mounted close to the transducer, and therefore remote from the terminal amplifier. The integrated circuit is called the "line-driver" part of the zero-drive system.

An input signal causes a change in the impedance of the FET. The terminal amplifier drives the line with a circuit exactly like a high-precision dynamically-controlled voltage regulator. Constant steady-state dc voltage is maintained on the line. Thus, when the impedance of the FET varies, the voltage on the line cannot vary. The current in the line must vary. This variation in current must ultimately be derived from the main power supply: a series resistor appropriately located can be used to extract a signal proportional to the current variation, and hence to the original signal.

The desired signal can now be conditioned, as required, in the main amplifier. For example, amplifier circuits may be needed to normalize the final output, power a front-panel meter, or drive a tape recorder and/or a galvanometer, etc.

Zero-drive input circuits can be arranged to deal with the input signal in the form of either voltage or charge.

The fact that the long line from terminal amplifier to line driver is driven by a regulated supply, means that the line is terminated by a very low dynamic impedance (a small fraction of an ohm). Hence, the system is impervious to many types of electrical pick-up.[2]

The zero-drive amplifier also solves for once and all the problem of cable triboelectric noise. Triboelectric noise is the component of electrical noise generated in a cable when the cable is mechanically flexed or vibrated. It is discussed in Appendix A. Very small cable motions produce this noise component. With charge or voltage amplifiers, it is a serious effect when fairly low-level signals are being amplified. Equation A-(16) illustrates the dramatic improvement when zero drive is used: the input impedance of the zero drive is 0.1 ohms, typically; for a conventional amplifier, an input impedance in excess of 10 megohms is required. The reduction in triboelectric noise in going to a zero drive system would therefore be in excess of 80 db.

Examination of Equations A-(17) and A-(19) indicates an even more dramatic effect in the triboelectric noise spectrum. With the charge or voltage amplifier, the triboelectric noise has its spectrum concentrated in the low-frequency region. In other words, not only is the total rms level of noise much higher than for the zero-drive amplifier, but the noise is confined to a narrow spectral region.

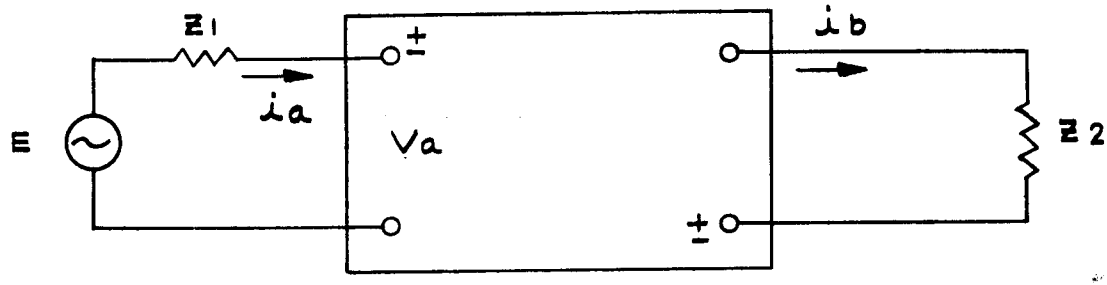

FIG. D-1: LINEAR TWO PORT

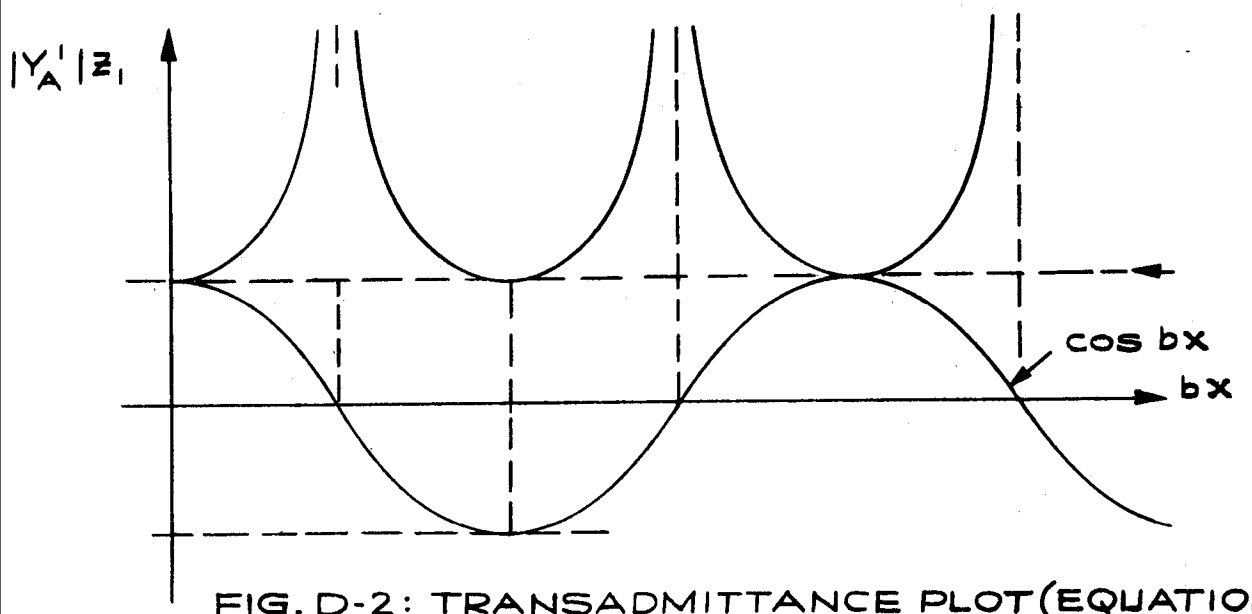

FIG. D-2: TRANSADMITTANCE PLOT (EQUATION D-(21)

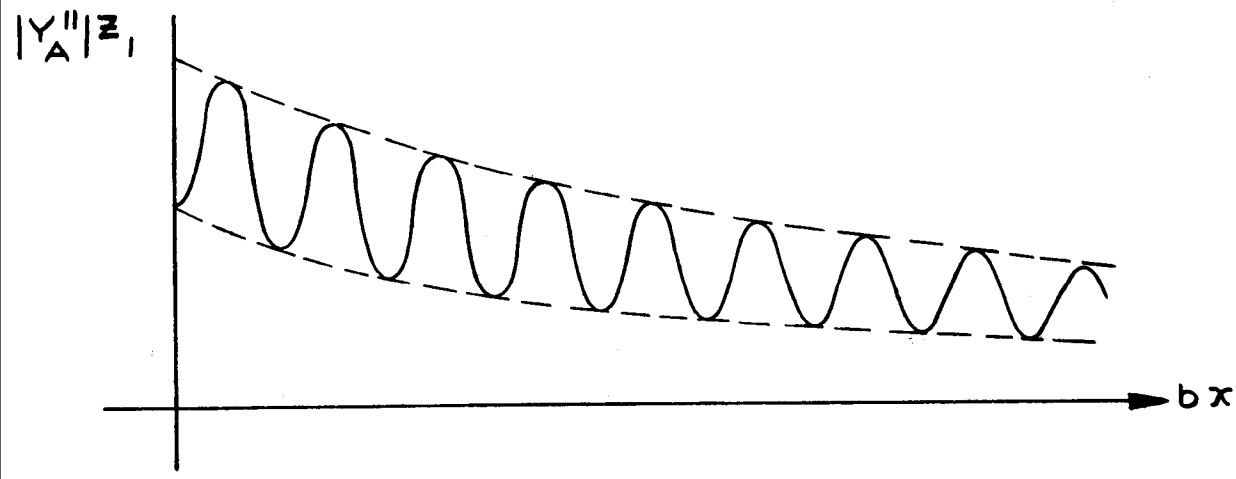

FIG. D-3: TRANSADMITTANCE PLOT (EQUATION D-(23)

If the amplifier is used as part of a vibration control system, this low-frequency region is displacement limited: thus, the acceleration signals are at levels that are significantly less than those obtained at the higher frequencies. A better noise level is needed to deal with acceleration signals at these low frequencies, not a worse one.

With the zero-drive system, the spectrum of the triboelectric noise is spread over a frequency range extending from zero Hz to well above the video: however, there is also a drastic decrease in spectral level that renders the noise completely ineffectual at any frequency.

The freedom from triboelectric noise means now that the amplifier system is freed from the use of expensive low-noise cable. Standard coaxial cables can be used without reservation, and the way is open to a wide extension of the application of the zero-drive principle to solve long-line data-transmission problems.

The zero-drive amplifier also has a very desirable effect on the level of conventional electrical noise. It has been shown experimentally that the noise level is almost independent of cable length.[2] This can be contrasted with the noise performance of the conventional charge amplifier, as discussed in Appendix B. Here the noise increases linearly with cable length: and thus, as the cable gets longer it very quickly becomes difficult to recover low-level signals with any accuracy.

The independence of zero-drive performance on the length and quality of the transmission cable makes the zero-drive principle worthy of investigation for use with piezoelectric signals approaching the video (i.e., covering the range: zero frequency to 2 mHz), even when the distance between transducer and amplifier is quite long. It offers a practical economical alternative to the complex and expensive telemetry schemes that must otherwise by employed.

HIGH-FREQUENCY PERFORMANCE WITH LONG LINES: MATCHING

Figures E-1, E-2 and E-3 summarize the exploratory tests carried out concerning the high-frequency long-line performance of the zero drive. They are explained in further detail in Appendix E.

Figure E-1 shows the results of the first exploratory experimental attempts to use the zero-drive system with frequencies beyond the audio. A basic audio system incorporating RG58/U coaxial line was used unmodified for the test. The curves of Figure E-1 plot the transfer-admittance, Y, defined by Equation D-(4). They confirm the theoretical results summarized in Equations D-(23) and D-(31): in particular, they verify the predicted resonances.

Similar resonant effects are obtained using charge or voltage amplifiers. Obviously, some form of impedance matching is essential. Unlike the latter amplifiers, the zero-drive amplifier readily lends itself to the necessary modifications.

For example, by matching the line-driver to the cable, the plot of Figure E-2 is obtained. The effect of the matching is obviously to remove the resonant peaks.

The same effect is produced by inserting a matching resistance at the amplifier end of the line: here a resistance Z_2, equal to Z_o, is placed in series with the line.

Simultaneously matching both ends of the line, in conformity with Equation D-(29), permits slight termination mismatches, without any resonant ripples whatsoever. Figure E-3 illustrates.

Note for each length of line, x, the frequency response is flat until the skin effect begins to exert its influence, as predicted by Equation D-(33). The experimental results indicate that

$$f_1 x^2 = 1.25 \times 10^{12} \qquad \text{Hz - ft}^2 \qquad (1)$$

Here, of course, f_1 is the highest frequency possible for a 1 db drop in the transfer-impedance characteristic.

EXTENSION OF FREQUENCY RANGE

Equation (1) permits a considerable extension of performance, in respect to both the frequency range and the length of line that can be handled. For example, if we have a shock pulse with significant frequency components up to 100 kHz, we can pass it over a line of RG58/U cable that is at least 3500 feet long. We can pass a 1 mHz signal over a line that is at least 1100 feet long.

Tests show that in practice, the signal wave-form will be preserved, even if it has frequency components significantly in excess of f_1. However, it is possible to extend the frequency range even further, by completely removing the droop represented by Equation D-(32). This can be done, using a frequency equalization network at the output of the terminal amplifier.

A typical equalization scheme is illustrated by the block diagram of Figure 2. An amplifier A has a four-pole equalization network, N, in its feed-back loop. The network, N, can be either passive or active in form. The circuit of Figure 3 illustrates the passive form; that of Figure 4 illustrates the active form. The networks are iterative in nature; the number of resistance and capacitance values chosen determines the closeness of the fit the transfer characteristic of network N to the curve of Equation D-(25).

The use of the isolation emitter-followers (EF) gives the circuit of Figure 4 a certain edge with regard to design flexibility. The curve of Equation D-(25) can easily be fitted with no more than ±0.3 db error.

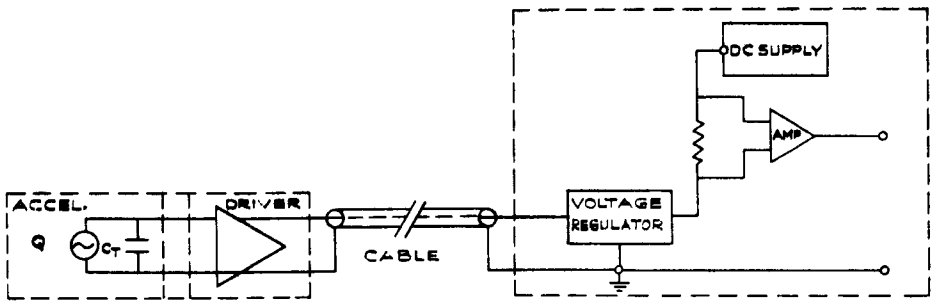

FIG. 1: ZERO DRIVE

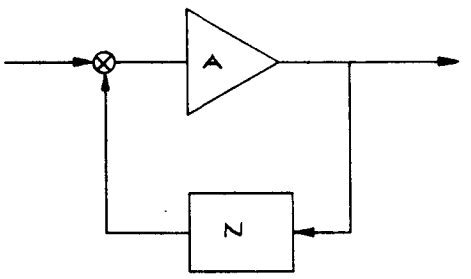

FIG. 2; FREQUENCY EQUALIZER

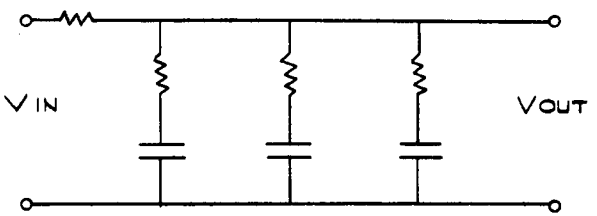

FIG. 3: NETWORK N

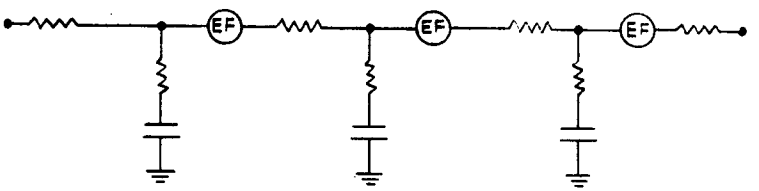

FIG. 4: NETWORK N (ACTIVE)

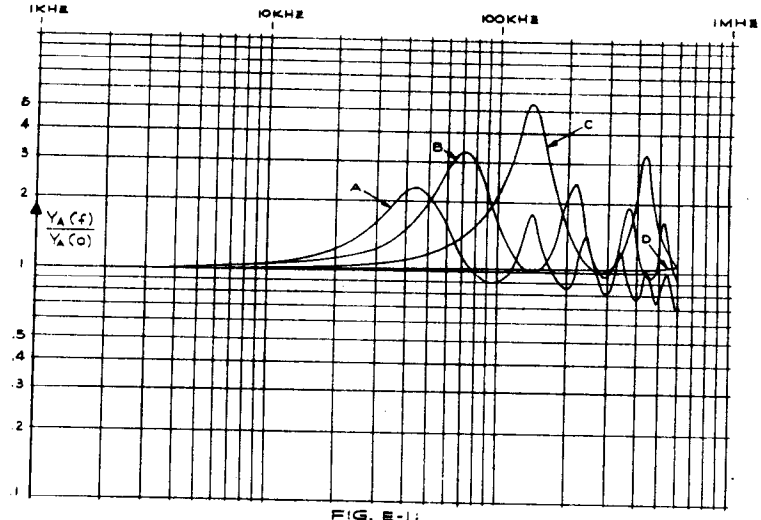

FIG. E-1:
EXPERIMENTAL RESULTS:
UNMATCHED SYSTEM

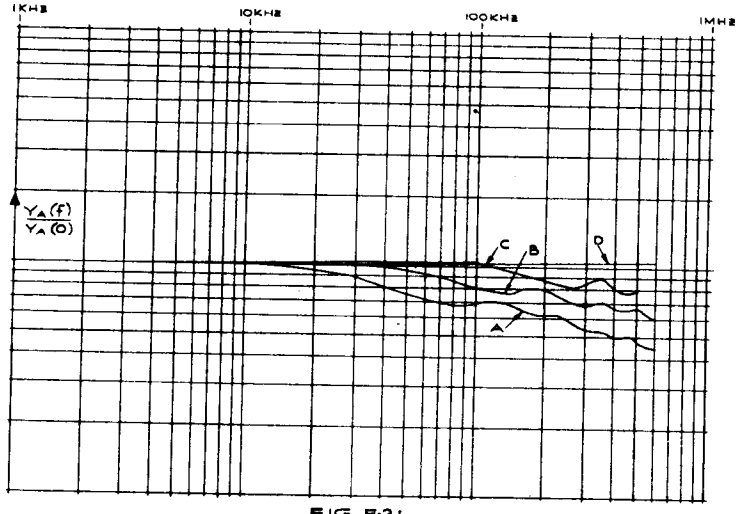

FIG. E-2:
RESULTS WITH SYSTEM
MATCHED AT ONE END

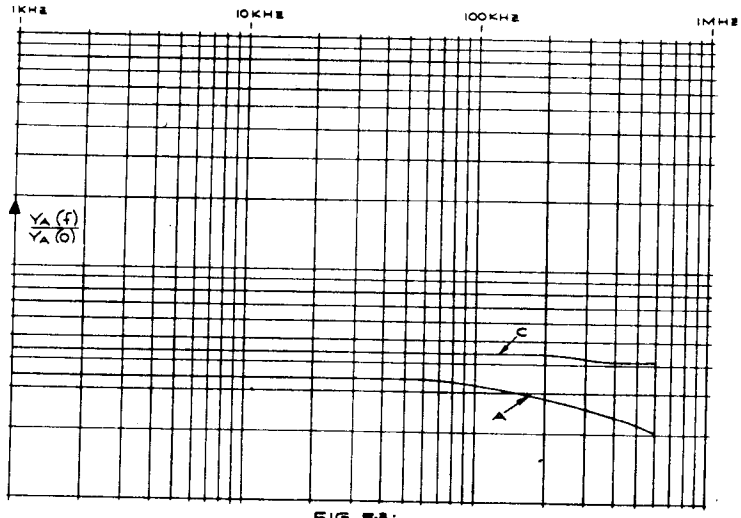

FIG. E-3:
RESULTS WITH SYSTEM
MATCH BOTH ENDS

The equalization circuits, of course, have some phase shift associated with their amplitude variations, while the amplitude change associated with Equation D-(25) has none. However, the circuits can be designed to confine the phase error introduced by them to d' degrees, where:

$$-10^{o} < d' < +10^{o} \qquad (2)$$

Equalization can be used to give quality transmission to frequencies in excess of $10f_1$. Typically, we can pass with little phase or amplitude distortion a signal containing frequencies up to at least 1.0 mHz over a line 5000 feet in length.

The equalization method is a good technique, since it does not involve any changes to either the coaxial line or the amplifier. It requires only the addition of a small circuit operating on the amplifier output signal.

CONCLUSION

The low output impedance of the terminal amplifier of a zero-drive system was originally aimed at reducing noise and pick-up in the range of frequencies associated with vibration and audio work, so that measurements with piezoelectric transducers would not be subject to the difficulties associated with charge and voltage amplifiers. This same low output impedance introduces a flexibility into the transducer-amplifier system, that opens the way to extending the upper end of the frequency range to the high ultrasonic region, even if long lines are needed between transducer and amplifier.

The usual method of transmitting wide-band ultrasonic or video signals is via an intermediate telemetry link, involving either PDM, PCM, or FM modulation. Ultra-high-frequency or microwave carriers are required. By means of the simple technique described here, it is possible in many cases to completely avoid the use of telemetry, with consequent savings in cost, system complexity, and maintenance.

REFERENCES

1. J.E. Judd, E.P. Moran, "Zero Drive-A New "Zero Impedance" Signal Conditioning Concept for Piezo-Electric Transducers", Instrument Society of America, Preprint No. P13-2-PHYMMID-67.

2. J.E. Judd, E.P. Moran, "A New Differential Zero-Drive System for Direct Wideband Audio Data Transmission over Standard Telephone Lines", M.B. Electronics, Inc., Reprint No. M68-1.

3. C.M. Harris, C.E. Crede, "Shock and Vibration Handbook", McGraw-Hill Book Company, New York, 1961.

4. T.A. Perls, "Electrical Noise from Instrumentation Cables Subjected to Shock and Vibration", App. Phys., Vol. 23, No. 6, p.p. 674-680, June, 1952.

5. T.A. Perls, "A Simple, Objective, Test for Cable Noise Due to Shock, Vibration or Transient Pressures", NBS Report No. 4094, May, 1955.

6. "Noise-Free Cable", N.B.S. Bulletin, March, 1952.

7. J.C. Slater, "Microwave Transmission", McGraw-Hill Book Company, New York, 1942.

8. L.G.H. Huxley, "A Survey of the Principles and Practices of Wave Guides", Cambridge University Press, Cambridge, 1947.

APPENDIX A

TRIBOELECTRIC NOISE

The basic work on triboelectric noise in cables was carried out by Perls, as part of an investigation into noise effects in piezoelectric instrumentation.[4] Triboelectric noise is generated when a cable is subjected to the flexing due to shock and/or vibration.[5] It arises whenever two conductors are separated by a dielectric, and one or both of these conductors can have a small motion with respect to the dielectric.[6] Even a very small relative motion can yield triboelectric noise, it only being necessary to have a temporary loss of electrical contact between dielectric and conductor over a small area. H.F. Richards reported as early as 1920 that an electrostatic charge is present on the surface of the dielectric with an opposite charge bound to the conductor. Under some conditions, potentials of the order of thousands of volts can be achieved.

Suppose separation occurs between one conductor of a coaxial line and its dielectric. Let s be the surface charge density generated (coulombs per square meter). Let A be the area of the affected surfaces. Let C_1 be the small air capacitance formed between the surface charge on the dielectric and the bound charge on the separated conductor. Let C_2 be the capacitance of the dielectric charge through the dielectric to the other conductor of the coaxial line. If Q_1 is the final charge on C_1 and Q_2 is the final charge on C_2, we see that:

$$Q_1 + Q_2 = sA \qquad A\text{-}(1)$$

Therefore, the charge that must pass through the input to any amplifier connected across the cable is Q_2:

$$Q_2 = \frac{sAC_2}{C_1+C_2} \qquad A\text{-}(2)$$

In consequence of the movement of this charge, a voltage, V^1, is generated across the input resistance, R, of the amplifier:

$$V^1 = \frac{Q_2}{C_o} \cdot \exp\left(-\frac{t}{RC_o}\right) \qquad A\text{-}(3)$$

where C_o is the parallel capacitance of the cable, the transducer and the amplifier input.

Now, if the cable is subjected to continuous mechanical motion, separation occurs at random times, with random effect. However, each time separation occurs, C_1 is much less than C. Hence we can write:

$$V(t) = \sum_{n=-\infty}^{+\infty} V_n^1 (t-t_n) \qquad A\text{-}(4)$$

where V^1 is contribution to the final output V due to the n-th separation.

$$V_n^1(t) = \frac{Q_{2n}}{C_o} \exp. \left(- \frac{t}{RC_o}\right) \qquad A\text{-}(5)$$

Q_{21}, Q_{22}, Q_{23}, etc., all represent independent random variables having the same probability distribution. Calculating the appropriate semi-invariants of V_n^1, and converting from these to statistical moments, we can now calculate $\overline{V}$ and v_o, where $\overline{V}$ is the average of V(t) and v_o is the rms level of V(t). It turns out that

$$\overline{V} = k\, R\, \overline{Q_2} \qquad A\text{-}(6)$$

where $\overline{Q_2}$ is the average of Q_2 and k is the number of separations per second.

$$\text{Also } v_o^2 = \frac{2k\,\overline{Q_2^2}\,RC_o}{C_o^2} + (k\,\overline{Q_2}R)^2 \frac{P}{kRC_o} \qquad A\text{-}(7)$$

$$\text{where } P = \frac{h}{1-h} \qquad A\text{-}(8)$$

$$h = \int_o^{oo} p(y) \exp - \frac{y}{RC_o} \cdot dy \qquad A\text{-}(9)$$

p(y) is the probability distribution of the interval of time, y, occuring between successive separations.

A representative form for p(y) is[4]:

$$p(y) = k \exp (- ky) \qquad A\text{-}(10)$$

Whence:

$$v_o^2 = \frac{kR}{C_o}\left[2\overline{Q_2^2} + (\overline{Q_2})^2 \cdot P\right] \qquad A\text{-}(11)$$

$$= \frac{kR}{C_o}\left[2\overline{Q_2^2} + kRC_o\,(\overline{Q_2})^2\right] \qquad A\text{-}(12)$$

The ac component of v_o, v, is given by:

$$v^2 = \frac{2kR}{C_o} \cdot \overline{Q_2^2} \qquad A\text{-}(13)$$

$$= 2\,kRC\,(\overline{V_o^2}) \qquad A\text{-}(14)$$

V_o is the initial voltage induced in the amplifier input by a single separation.

From Equation A-(14):

$$v = \sqrt{2kRC_o} \cdot \sqrt{V_o^2} \qquad A\text{-}(15)$$

The quantity v represents the triboelectric noise passed through the instrumentation amplifier. Here, of course, the quantity C_o actually includes the transducer capacitance and input capacitance of the amplifier: if we assume for comparison's sake that the amplifier input capacitance is negligible, and that we are working with the same cable and transducer, we can write that the improvements in S/N ratio of the zero-drive amplifier over the conventional high-input charge or voltage amplifier is given by r in:

$$r = \sqrt{\frac{R}{R_a}} \qquad A\text{-}(16)$$

where R is the input resistance of the zero drive and R_a is the input resistance of the conventional amplifier.

Turning now to the power spectral density, W(f), it can be shown that W(f) is given by:

$$W(f) = \frac{4\,RC_o\,v^2}{1 + (2\pi fRC_o)^2} \qquad A\text{-}(17)$$

At frequencies less than $1/(2\pi RC_o)$, W(f) reduces to:

$$W_L(f) = 4\,RC_o v^2 \qquad A\text{-}(18)$$

$$= 8\,kR^2\,C_o^2 \cdot \overline{V_o^2} \qquad A\text{-}(19)$$

APPENDIX B

NOISE IN CHARGE AMPLIFIER SYSTEM

For definiteness the following discussion relates to the use of a charge amplifier with a piezoelectric accelerometer. The conclusions are easily adapted to the charge amplifier used with other types of piezoelectric transducer.

For the present purpose, the schematic of Figure B-1 is suitable. Here C_L represents the total capacitance presented at the amplifier by the coaxial line and the piezoelectric transducer.[3]

The charge amplifier itself is represented by the combination of feedback capacitor, C_F, plus high-gain amplifier, A.

If H is the gain of the amplifier A, the output noise level is given by N_o in:

$$\frac{N_o}{N_A} = \frac{C_F + C_L}{C_F\,H}\left[1 + \frac{C_F + C_L}{C_F\,H}\right]^{-1} \qquad B\text{-}(1)$$

N_A is the level of the internal noise generated in A; N_A is the level of this noise measured at the output of A.

H is usually quite large, so that Equation B-(1) reduces to:

$$N_o = \frac{N_A}{H}\left[1 + \frac{C_L}{C_F}\right] \qquad \text{B-(2)}$$

The quantities N_A, H, and C_F are set by the amplifier. The quantity (N_A/H), of course, is the amplifier noise referred to its input. C_L is given by:

$$C_L = C_T + xC \qquad \text{B-(3)}$$

where x is the length of cable. The noise level of a charge-amplifier system, therefore, inherently reduces to the form:

$$N_o = K_1 + K_2 \cdot x \qquad \text{B-(4)}$$

APPENDIX C

RG 58/U COAXIAL CABLE

The constants per foot of RG58/U are:

R = 0.014 ohms
C = 30 mmfd
G = 0
L = 0.078 microhenrys
Z_o = 50 ohms
$f_T = \frac{R}{2\pi L}$ = 28.6 kHz
D = diameter of inner conductor
= 0.020 in.

APPENDIX D

THEORY OF LONG-LINE EFFECTS OF THE ZERO-DRIVE

A coaxial line can be represented by the linear two-port of Figure D-1. Currents and voltages are defined in the Figure: the relationship between the input voltage and current (V_a, i_a) and the output voltage and current (V_b, i_b), for the cable only, is given as follows:[7]

$$V_a = Z_{aa}\, i_a + Z_{ab}\, i_b \qquad \text{D-(1)}$$

$$V_b = Z_{ab}\, i_a + Z_{bb}\, i_b \qquad \text{D-(2)}$$

The Thévenin equivalent circuit for the line-driver is represented by the voltage, E, and series impedance, Z_1; while Z_2 represents the dynamic impedance of the amplifier.

The output current i_b is the means whereby the data intelligence is transferred. Hence, we are interested in the transfer-admittance:

$$Y = -\frac{i_b}{E} \qquad \text{D-(3)}$$

Combining Equation D-(1), et seq., we get:[8]

$$Y = \frac{Z_{ab}}{Z_o^2 + Z_1 Z_2 + Z_{aa}(Z_1+Z_2)} \qquad \text{D-(4)}$$

where

$$Z_o^2 = Z_{aa} Z_{bb} - Z_{ab}^2 \qquad \text{D-(5)}$$

$$= Z_{ab}^2 (\sinh cx)^2 \qquad \text{D-(6)}$$

$$Z_{aa} = Z_o \coth cx \qquad \text{D-(7)}$$

$$= Z_{bb} \qquad \text{D-(8)}$$

$$c = a + jb \qquad \text{D-(9)}$$

$$c^2 = (R+jLw)(G+jwC) \qquad \text{D-(10)}$$

$$Z_o^2 = \left(\frac{R+jLw}{G+jCw}\right) \qquad \text{D-(11)}$$

In the above, x is the line length. Z_o is the characteristic impedance of the line. The parameter c is the propagation constant of the line, a is its attenuation constant, and b its wavelength constant. The line parameters are given in terms of the line properties, R,L,G,C, which represent, respectively, the unit length series resistance, series inductance, leakage conductance and shunt capacitance. For most lines, G can be neglected.

At low frequencies,

$$Lw \ll R \qquad \text{D-(12)}$$

and the constants given by Equations D-(5) to D-(11) reduce to:

$$c^2 = jwRC \qquad \text{D-(13)}$$

$$Z_o^2 = \frac{R}{jCw} \qquad \text{D-(14)}$$

$$a = b = \sqrt{\frac{RCw}{2}} \qquad \text{D-(15)}$$

Finally, Y reduce to Y_L:

$$Y_L = \frac{1}{Rx + Z_1 + Z_2} \qquad \text{D-(16)}$$

At high frequencies,

$$Lw \gg R \qquad \text{D-(17)}$$

and the constants given by Equations D-(5) to D-(11) reduce to:

$$a = \frac{R}{2Z_o} \qquad \text{D-(18)}$$

$$b = w.\sqrt{LC} \qquad \text{D-(19)}$$

$$Z_o = \sqrt{\frac{L}{C}} \cdot \left(1 - \frac{jR}{2wL}\right) \qquad \text{D-(20)}$$

When the frequency becomes high enough, we can assume R is zero in Equation D-(20).

The transition frequency region, where Lw cannot be ignored, but where (R/Lw) is not a fraction less than unity, is a difficult region to analyze. Fortunately, the frequency region of primary interest here is that given by Inequality D-(17). Equation D-(4) is solved for a variety of conditions for this frequency region.

Condition A: $Z_2 = 0$, $Z_1 \neq 0$, $Y = Y_A$.

Assume for the moment that the attenuation constant, a, is zero: Y_A is now Y_A^1

$$Y_A^1 = \frac{1}{Z_1 \cos bx} \qquad \text{D-(21)}$$

Y_A^1 is plotted in Figure D-2, Note the infinite resonance peak at

$$bx = \pi, 3\pi, 5\pi, \ldots \qquad \text{D-(22)}$$

If we have a non-zero value for the attenuation constant, Y_A is now:

$$\left|Y_A'\right| = \frac{I}{Z_1\left[\cos^2 bx \cosh^2 ax + \sin^2 bx \sinh^2 ax\right]^{1/2}} \qquad \text{D-(23)}$$

$\left|Y_A''\right| \cdot Z_1$ is plotted in Figure D-3.

If the input impedance is matched; i.e., if

$$Z_1 = Z_o \qquad \text{D-(24)}$$

then Y_A becomes Y_{AM}:

and $$Z_o \cdot Y_{AM} = e^{-ax} \qquad \text{D-(25)}$$

Condition B: $Z_2 = Z_o$, $Z_1 \neq 0$

Here $$Y = Y_B = \frac{I}{[M]\cos bx + j[N]\sin bx} \qquad \text{D-(26)}$$

where $$[M] = Z_o e^{ax} + Z_1 (1 + \cos ax) \qquad \text{D-(27)}$$

$$[N] = Z_o e^{ax} + Z_1 \sinh ax \qquad \text{D-(28)}$$

A plot of Y_B reveals an attenuation law of the same form as that shown in Figure D-3.

If Z_1 is now matched to Z_o; i.e., if

$$Z_1 = Z_2 = Z_o = \sqrt{\frac{L}{C}} \qquad \text{D-(29)}$$

Then Y_B becomes Y_{BM}:

$$Y_{BM} = \frac{1}{2Z_o} e^{-ax} \qquad \text{D-(30)}$$

Skin Effect: Skin effect alters the value of R with frequency, so that the plots Y_A, Y_A^1, Y_{AM}, Y_B and Y_{BM} actually differ from those predicted by the equations given above. The effect is associated with the attenuation properties of the coaxial line:[8] the constant a becomes a^1:

$$a^1 = \frac{RD}{20 \cdot Z_o} \cdot \sqrt{f} \qquad \text{D-(31)}$$

For a given length of line, Y_{AM} and Y_{BM} are constant, until the frequency gets high enough to change the attenuation thus

$$2Z_o\, Y_{BM} = \exp\left\{-\frac{RD}{20\, Z_o}\sqrt{f}\cdot x\right\} \qquad \text{D-(32)}$$

The point where the attenuation starts to drop off with frequency depends on the length of the line. The -1 db point is given by frequency f_1 in:

$$f_1 x^2 = 5.33\left\{\frac{Z_o^2}{R^2 D^2}\right\} \qquad \text{D-(33)}$$

Thus, if we double x, f_1 is reduced by one quarter.

APPENDIX E

DISCUSSION OF EXPERIMENTAL RESULTS

The curves of Figure E-1, E-2, and E-3 summarize the experimental work carried out on a standard zero-drive system, to see how high in frequency such a system can be made to function. The effects of frequency equalization are ignored here, since the purpose is to illustrate the basic physical phenamena involved. An equalization scheme (see Figure 2), of course, can easily be used to extend the frequency range by at least a decade. The cable employed was RG58/U. Its properties are summarized in Appendix C. The curves are effectively plots of the transfer-admittance, Y, Equation D-(4).

Figure E-1 plots the response of an unmodified zero-drive amplifier. The line-drive impedance, Z_1, is much larger than the characteristic impedance of the line, Z_o. (Z_1 = 2000 ohms, Z_o = 50 ohms). The amplifier impedance, (Z_2) is effectively zero. Curves A, B, and C are plots of Y corresponding to line lengths, x, as given in Table E-1. These plots correspond to the theoretical plots of Equations D-(21) and D-(23).

TABLE E-1

Curve	Line length (x) in feet
A	3000
B	2000
C	1000
D	25

Note that the horizontal asymptote at the low-frequency end of the plots has a smaller intercept on the ordinate axis, as the line lengths increased. This effect, of course, is as predicted by Equations D-(16) and D-(23).

With increased line length, a given value for the quantity bx is reached at a lower value of frequency.

(See Equations D-(19) and D-(21).) Hence the resonant effects occur sooner for curve A than for curve C.

Figure E-2 illustrates what happens when a matching resistor is put in parallel across the line-driver output. Now Equation D-(24) is satisfied. The impedance Z_1 is obtained by using a resistor which is ac-coupled across the line-driver output. The small ripples on the plot are the result a slight mismatch between Z_1 and Z_o. Otherwise the predictions of Equations D-(25) and D-(31) are completely satisfied. Curves A, B, and C follow Table E-1.

Figure E-3 is for full matching at each end of the cable. Equation D-(29) is satisfied. Curves A, B, and C follow Table E-1, once again. These curves are completely flat, except for the droop-off at high frequencies due to skin effect. Once again, the signal attenuation increases with increased line length. Equations D-(16) and D-(30), of course, predict this. For example,

$$Y_L = \frac{1}{2Z_o + Rx} \qquad \text{E-(1)}$$

which decreases as x increases. Also, if ax is small, as it is in this case:

$$Y_{BM} = \frac{1}{2Z_o}(1-ax) \qquad \text{E-(2)}$$

From Equation A-(18):

$$Y_{BM} = \frac{1}{2Z_o\left[1 + \frac{Rx}{2Z_o}\right]} \qquad \text{E-(3)}$$

Hence, $$Y_L = Y_{BM} \qquad \text{E-(4)}$$

and the plot for a given value of x is flat with frequency. The plot of Figure E-3 confirms Equation E-(4), Skin effect, of course, effects the plot at the higher frequencies.

68-503

DIFFUSED SILICON DIAPHRAGM PRESSURE TRANSDUCERS

Norman Zinker, Member
Manager of Engineering
Fairchild Camera and Instrument Corporation
Controls Division, Transducer Plant
Mountain View, California

ABSTRACT

The properties and characteristics of a diffused silicon diaphragm pressure transducer are presented. Emphasis is placed upon the design goals, problems, method of fabrication, need, utilization and areas of improvement. The diffused diaphragm pressure transducer is one of the few devices specifically developed as a transducer and not the by-product of some other requirement. The simplicity of design and mass production capabilities make it a unit ideally suited for the industrial-commercial market due to a low selling price with built-in reliability and dependability. In addition, the unit can be packaged to meet military requirements and will have a strong appeal for the aerospace and aircraft industry requiring these same characteristics.

INTRODUCTION

During the past thirty-five years strain gages have emerged from a laboratory curiosity to an indispensable tool of the structural analyst.

Considerable development was necessary before the strain gage was capable of reaching this position of importance. After the introduction of the unbonded wire strain gage there were four major improvements or additions: direct mounting of the wire gage to the surface being measured, premounted wire on suitable carriers, the foil strain gage and the semiconductor gage.[1]

These improvements and innovations have had a considerable impact on the technical society. Many new and varied uses were quickly found for these devices; one of the most significant has been in transducer technology. Very few of the developments or improvements have been made with the transducer specifically in mind; therefore, it was only a by-product of other needs or requirements. Fortunately, these by-products had yielded some very fine results for transducer designs. The time has arrived when there no longer appears to be any major improvements coming in strain gage technology. But the requirements for improved transducers and new transducer technology has grown at an ever increasing pace, both for the military as well as the industrial user: the military user in the more exotic spacecraft and aircraft requirements, and the industrial user in trying to keep up with the ever demanding requirements of automation and computer input needs as well as the ever expanding consumer market with its vast potential for many and varied products.

The transducer designer has had to look internally for his next improvements in technology and design. Although this need is perhaps more apparent for the strain gage based transducer, it is equally true for those using the other popular techniques for transduction such as capacitive, differential transformer and variable reluctance. The designers are dependent upon improvements by the various manufacturers of the basic components of their transducers, improvements which may be metalurgical, physical or chemical.

With these facts in mind, and after considerable development, Fairchild Controls introduced the all silicon diffused diaphragm FPT series transducer in 1962. (See Figure 1.) The design goals consisted of simplicity of mechanical design, no moving parts, no linkages, small, light weight, high output and medium price. These goals, it was believed, were in keeping with the requirements of our customers and well within the manufacturing capabilities of Fairchild Controls due to its close proximity and corporate affiliation with Fairchild Semiconductor.

FPT SERIES PRESSURE TRANSDUCER

Design

The FPT transducer is a semiconductor strain gage based pressure sensing device. The sensing portion of the transducer is a planar diffused silicon pressure diaphragm which has four diffused strain sensing resistive elements. These elements are laid out in the standard four-active-arm Wheatstone bridge. When pressure is applied to the silicon diaphragm, a change of resistance in the strain-sensors is produced due to the piezoresistive effect of the semiconductor material.[2], [3] A voltage is thus produced at the output terminals of the Wheatstone bridge which is directly proportional to the applied pressure and excitation voltage.

Superior numbers refer to similarly-numbered references at the end of this paper.

Operation

The FPT transducer has two strain sensing resistive elements located in a region of tensile strain, thus causing the resistance to increase by an amount ΔR when pressure is applied. (See Fig. 2.) The remaining two strain sensing resistive elements are located in a region of compressive strain, thus causing the resistance to decrease by an amount ΔR.[4], [5] The output voltage, as a result of pressure-induced strain, is given by the following equation:

$$E_{OUT} = E_{IN} \frac{\Delta R}{R} \quad (1)$$

where E_{OUT} equals output voltage in volts

E_{IN} equals input voltage in volts

ΔR equals resistance in ohms

R equals unstrained resistance of bridge elements in ohms

Another method is shown in Figure 3 in which the transducer is excited by a constant current source I_{IN} amperes.

The output now, as a result of pressure induced strain, is given by the following equation:

$$E_{OUT} = I_{IN} \Delta R \quad (2)$$

Temperature

Of all the environmental conditions to which the transducer may be subjected, temperature dependence is the most significant since shock, vibration and acceleration have negligible effect on a diffused diaphragm transducer. In the FPT transducer both the input and output impedance are equal in value to the unstrained resistance R of one of the strain sensitive bridge resistors. When the unit is pressured this relationship does not change. With temperature the resistance values do change. This temperature dependence of resistance is shown in Figure 4. Sensitivity, which is defined as the electrical output less the zero offset divided by the excitation voltage at full scale pressure, is dependent upon temperature as follows:

With constant voltage excitation it can be seen from equation (1) that sensitivity varies with temperature as

$$\frac{\Delta R_{F.S.}}{R}$$

therefore

$$\frac{E_{OUT}}{E_{IN}} = \frac{\Delta R_{F.S.}}{R}$$

where E_{IN} is held constant through temperature. A typical plot of E_{OUT}/E_{IN} is shown in Figure 5.

With constant current excitation it can be seen from equation (2) that sensitivity now varies with temperature as

$$\Delta R_{F.S.}$$

therefore

$$\frac{E_{OUT}}{I_{IN}} = \Delta R_{F.S.}$$

where I_{IN} is held constant through temperature. A typical plot of E_{OUT}/E_{IN} is shown in Figure 6.

From Figure 5 and Figure 6 it is evident that the sensitivity *versus* temperature curve can be optimized even further. This can be accomplished by the proper choice of resistors in series with a constant voltage source or in parallel with a constant current source.

New Design

The introduction of the diffused diaphragm transducer showed the typical new product curiosity. It soon became apparent that the price and accuracy were not overshadowed by the small size, light weight, high output and frequency response; thus, the unit had less than the desired degree of success.

At this point the diffused diaphragm transducer was reevaluated. The original design goals were found to be lacking so a new set of goals would have to be decided upon. From the many inquiries received from our sales people as well as potential customers over the past years, the following design goals and markets were chosen.

Industrial customers are looking for a more reliable, rugged, low-cost, dependable, accurate transducer. These requirements and customers then became our goals and the necessary changes to the FPT series transducer were begun. The first goal was to reduce the cost. A cost reduction was achieved by relaxing certain parameters, redesigning and simplifying the housing. (See Figure 7.) The new design was well accepted by the industrial customer who was willing to pay a slightly higher price than the other transducers presently being used, as long as dependability could be guaranteed, since the other types of transducers do not survive adverse environmental conditions. With some degree of assurance that our goals and markets were in the right direction, it was decided to proceed further to improve and reduce cost of this series transducer.

In order to further improve the FPT series transducers in performance as well as further lower the price, the fabrication of the diffused Wheatstone bridge was investigated. The original mask design for the diffused transducer was completed in 1960; since then the dynamic semiconductor manufacturers have come a long way in improving growing silicon ingots, photographic techniques, X-ray technology and silicon processing, as well as use and development of epoxies to be used with semiconductors.

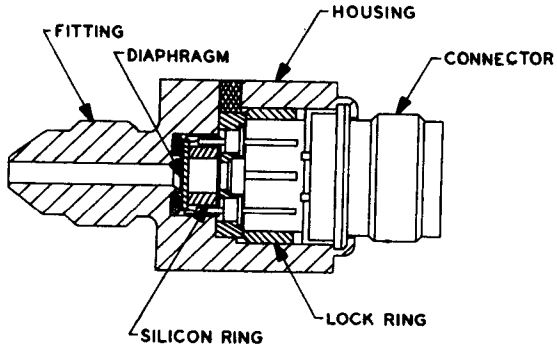

Figure 1: FPT - Silicon diffused diaphragm transducer

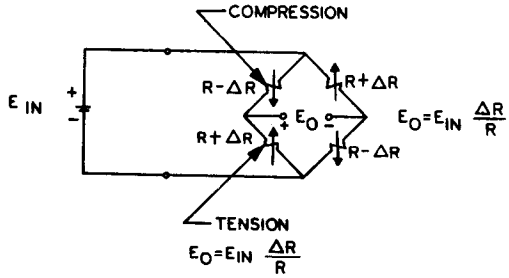

Figure 2: Wheatstone bridge (during pressurization) excited by constant voltage source.

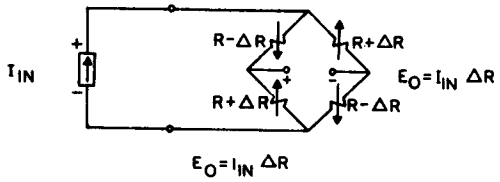

Figure 3: Wheatstone bridge excited by constant current source.

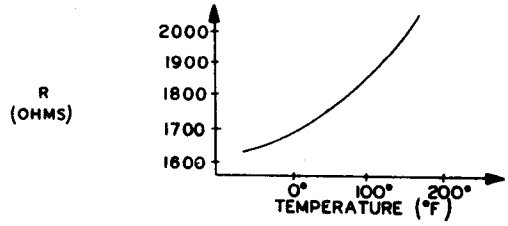

Figure 4: Bridge impedance *vs* temperature for typical FPT-series Pressure Transducer

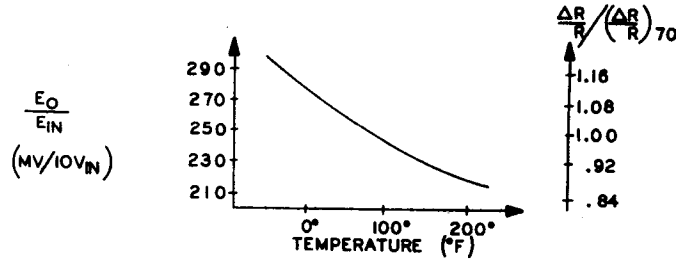

Figure 5: Sensitivity *vs* temperature with constant voltage (10 volts) applied to input

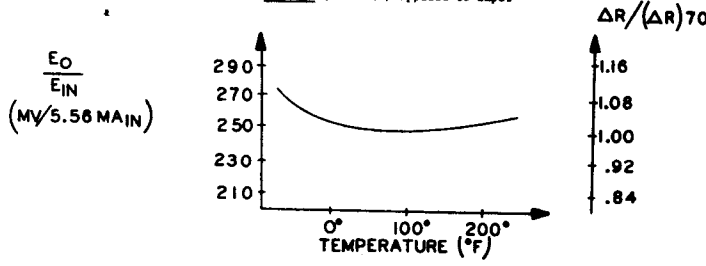

Figure 6: Sensitivity *vs* temperature with constant current applied to input